
Article:
Lewis, R. orcid.org/0000-0002-4300-0540, Trummer, G., Six, K. et al. (5 more authors) (2023) Leaves on the line: characterising leaf based low adhesion on railway rails. Tribology International, 185. 108529. ISSN 0301-679X

https://doi.org/10.1016/j.triboint.2023.108529

Tribology International 185 (2023) 108529

Contents lists available at ScienceDirect

Tribology International

journal homepage: www.elsevier.com/locate/triboint

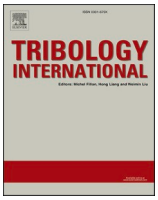

Leaves on the line: Characterising leaf based low adhesion on railway rails

R. Lewis [a,*], G. Trummer [b], K. Six [b], J. Stow [c], H. Alturbeh [c], B. Bryce [c], P. Shackleton [c], L. Buckley Johnstone [a]

[a] The University of Sheffield, Department of Mechanical Engineering, UK
[b] Virtual Vehicle Research GmbH, Graz, Austria
[c] Institute of Railway Research, University of Huddersfield, UK

ARTICLE INFO

Keywords:
Wheel/rail interface
Creep force
Low adhesion
Leaf layers

ABSTRACT

Work was carried out to generate wheel/rail interface creep force data with the presence of leaf contamination. To enable this. the HAROLD full-scale wheel/rail test rig was upgraded to give friction measurement capability and methods for creating leaf layers were also developed.

A unique dataset has been created not previously available for full-scale test conditions and leaf layers. The work has shown the importance of the shear induced in the brake tests for creating the black, well-bonded leaf layer. It was found in the tests that ultra-low adhesion was achieved in all tests with leaves regardless of load applied and speed. The friction was also low for a number of braking events, even when the layer had been partially removed.

1. Introduction

Low adhesion causes many problems during the Autumn period for train operation due to leaf fall and the creation of the well-known black, well bonded, slippery layer on the rail head (see Fig. 1). This causes many problems for safety as train braking is affected and incidents such as signals passed at danger (SPADs) and station overruns occur. Traction is also affected which impacts on train performance and can lead to timetable changes being imposed and passenger dissatisfaction rising.

There have been a large number of laboratory based studies of low adhesion due to leaf contamination, many of which have been summarised in a comprehensive review [9]. Tests showed exceptionally low levels of friction (0.01–0.02, compared to 0.03–0.09 typically required for normal service brake application) can occur, as would be expected, and provided a benchmark for testing mitigation products such as traction gels [12]. They have also been useful for running carefully controlled tests to assess the chemical reactions occurring in the contact between the wheel and the rail. Such tests have been used to identify different leaf components that may be contributing to the low friction problem, such as tannins [4,18], or pectin [2], as well as the role of iron oxide from the rail steel itself [8]. Small-scale research has shown that temperature is important for layer creation and bonding [7,10] which in turn is strongly dependent on speed, and slip in the contact. However, small scale testing can rarely achieve speeds representative of those for trains in service. It is clear from field testing, that braking events change the nature of the layer from the initial green/brown mulched leaf form to the well bonded black layer that causes low adhesion [11]. Despite the fact it is hard to simulate braking events in a small-scale test set-up, very little laboratory research on the characteristics of leaf-based low adhesion has been carried out at full-scale.

A number of modelling approaches have been developed for creating creep force - creepage curves for wheel-rail contact, some of which are able to incorporate the effects of third body materials [17]. The Extended Creep Force model, for example, has been parameterised using creep force relations measured in high pressure torsion testing to allow full-scale behaviour with sand [15] or top-of-rail friction modifiers [5,13] in the interface. The water induced low adhesion creep force model (WILAC) was recently developed for predicting reduced friction levels when small amounts of water are present in the wheel-rail contact together with iron oxides which create a slippery paste, resulting in the so-called “wet-rail” phenomenon [16]. The model was developed through a parameterisation process using creep curve results from full-scale testing using a rig incorporating an actual wheel running against a disc with a rail profile [1]. To date, no model has been developed, however, that accounts for leaves in the contact.

There was a clear need to carry out leaf layer creation and friction testing at full-scale conditions to allow braking and testing at representative speeds and loads. These would help in understanding leaf layer

* Corresponding author.
E-mail address: roger.lewis@sheffield.ac.uk (R. Lewis).

https://doi.org/10.1016/j.triboint.2023.108529
Received 5 January 2023; Received in revised form 1 March 2023; Accepted 16 April 2023
Available online 17 April 2023

formation and evolution as well as providing a possible test approach for assessing different types of mitigation technologies. Such tests could also provide the data necessary for developing a creep-force model for predicting friction behaviour with leaf contamination in the wheel/rail interface based around the approaches and models described above.

The aim of the work was to generate creep-force data for leaf contaminated conditions to be used to develop the WILAC model further to take account of these conditions. To generate the curves leaf layer brake tests were to be carried out on the Huddersfield Adhesion and Rolling Contact Laboratory Dynamics Rig (HAROLD) full-scale test rig with leaf layers. Initially the rig had to be upgraded to achieve such measurements and leaf layer generation protocols had to be developed. Benchmark tests were also carried out in dry and wet conditions.

2. Experimental details

2.1. Test apparatus

The HAROLD rig is a full-scale test machine capable of accommodating a railway bogie and running one axle of the bogie on a 2 m diameter rail roller at speeds up to 200 km/h. Forces can be applied to the secondary suspension by means of hydraulic actuators, allowing the vertical wheel-rail contact forces to be varied. A general view of the HAROLD test rig is shown in Fig. 2.

The tests used a Y25 freight bogie positioned with the leading wheelset on the rail roller. The bogie was mounted on the HAROLD rig with the test wheelset secured by its axle boxes to the load table. One side of the tested wheelset was jacked up to give a small clearance to the rail roller as shown in Figs. 3 and 4. This meant that it was only necessary to produce a contaminant film in one wheel-rail contact and avoided complications which might arise in interpreting the results if different friction conditions were present between the two wheels on the wheelset. All braking was carried out on the jacked (non-contacting wheel). Lifting the wheel in this way had a small influence on the contact conditions of the opposite wheel due to the small increase in wheelset roll angle. The magnitude of the effect depends on the geometry of the contacting bodies. In these tests, the position of the jacked wheel caused an increase in contact patch area, and consequent reduction in contact stress of around 13% when compared to the un-jacked wheel positioned centrally in the track (roller) gauge. This was considered to be of a similar order to the changes in contact conditions resulting from the normal lateral movements of the wheelset within the track gauge in service. and was therefore considered acceptable.

The Y25 bogie is equipped with tread brakes where the brake block acts on the running face (tread) of the wheel. As the brake blocks would have a cleaning effect on the test wheel, a device was designed to clamp the brake linkage on all wheels except the jacked/braked wheel. This ensured that the braking force was distributed as normal through the linkage whilst only actually applying a braking force to the jacked wheel. The brake linkage shorting mechanisms is shown in Fig. 5.

The rotating rail roller is driven by a motor, which in turn drives the wheel in contact. Roller and wheel speeds are measured by encoders on each shaft. The normal load is measured by two load cells located in the supports for the rail rollers. The longitudinal loads are measured by tension-compression load cells between the axle box and securing brackets as shown in Fig. 6. Vertical load was applied through the bogie bolster.

A simple wheel slide protection (WSP) system was developed to monitor the creepage and release the brake when it reaches a predefined configurable creepage threshold.

2.2. Test conditions

For this work typical British mainline wheel/rail interface conditions were targeted in terms of contact stress and vehicle speed. The wheel loads used and their corresponding Hertzian contact stresses are shown in Table 1. Note that the loads reported later in Section 3 sometimes differ from those shown in Table 1, but represent those actually recorded

Fig. 1. Leaf Layer Generated in the Field by Rolling a Vehicle over Leaves Applied to the Rail: (a) 0 Passes, (b) 2 Passes (c) 5 Passes and (d) Post-Braking Appearance [11].

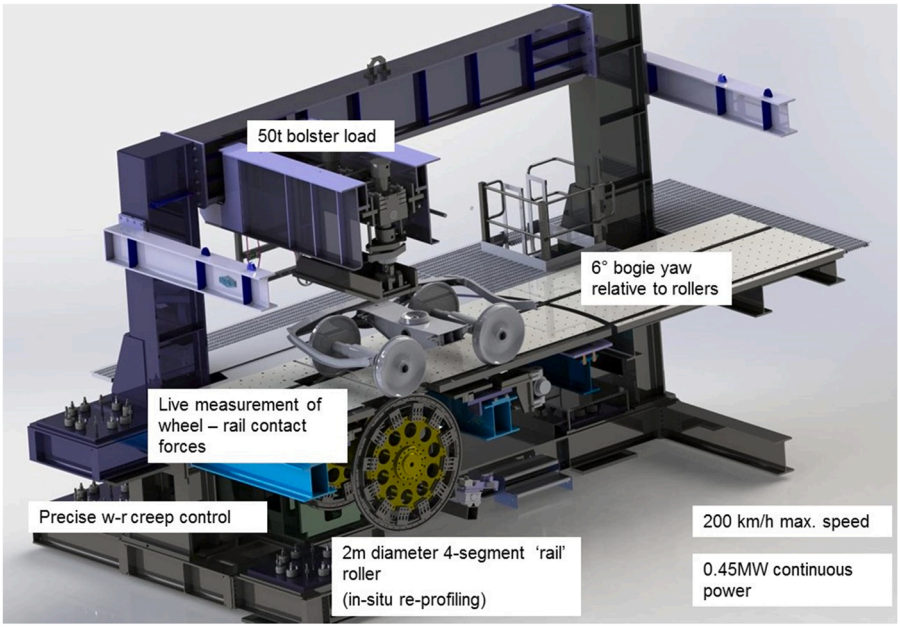

Fig. 2. General View of the HAROLD Test Machine.

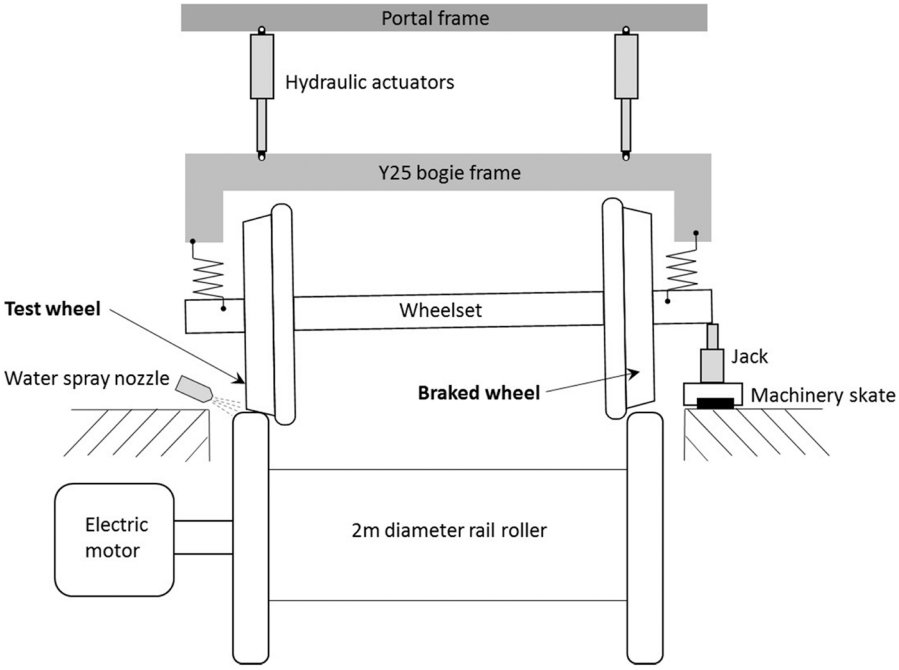

Fig. 3. Test Set-up Schematic.

during the tests. Speeds up 30 m/s (72 km/h) were used. The dry test conditions and those for the various contaminants are shown in Table 2. For contaminated conditions it was possible to test at higher loads as adhesion reduced. The load limit for dry conditions of 21 kN was dictated by the maximum brake force that can be applied, also seen in other full-scale test rigs of this nature (see for example [19]]).

2.3. Test methodology

2.3.1. HAROLD brake test process

The HAROLD rig test has an input file to define the variation of applied braking force with time. Fig. 7 shows a graphical representation of a test procedure that was used in the HAROLD input file for these tests. The roller is initially run at constant speed (A-B) and then the brake pressure ramped up to the predefined maximum pressure (B-C) and held constant (C-D) only if no wheel slide occurs during brake application. If wheel slide occurs at any point in the braking cycle a simple wheel slide protection system (WSP) releases the brakes when a preset creepage is reached and reapplies them once the wheel has accelerated to match the speed of the roller. Creepage limits were set below the maximum desired value of 100% in order to protect the wheel from flats.

It should be noted here that creepage control, to maintain a constant value of creepage was considered, but was not possible because the pneumatic system is too slow and there would have been a high likelihood of wheel flats occurring. Fig. 8 shows the process of running a

Fig. 4. Jacked Wheel.

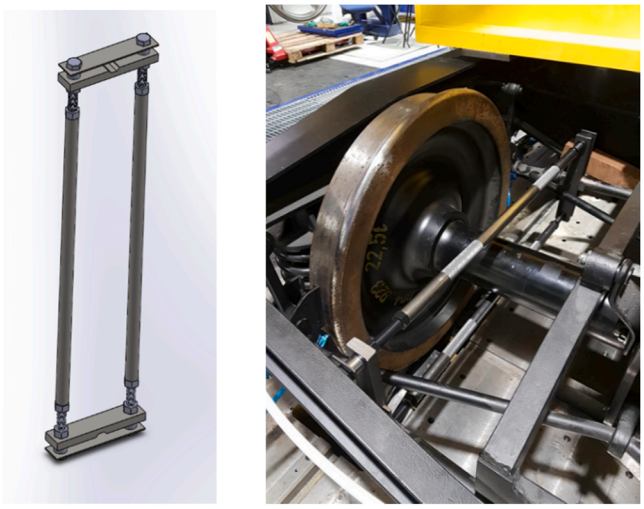

Fig. 5. Brake Shorting Mechanism Installed on the Bogie.

creep curve measurement using HAROLD. The time to free rolling is speed dependent. The brake application occurs over 50 s, however the maximum brake force chosen varied depending on the normal load condition being tested and the assumed maximum friction force.

2.3.2. Leaf layer creation

Several methods were trialled to generate a reliable leaf film across the two surfaces in contact. The first was to pre-prepare a "strip" of dry Sycamore leaves, held together with paper adhesive tape, that were fed into the wheel/rail interface. This was successful, but it was found that feeding broken up leaves into the wheel-rail contact using a scoop achieved the same leaf layer more quickly (see Fig. 9). Leaves were "dry" with uncontrolled and unknown water content during preparation of the leaf layer on the surfaces of the wheel and the rail roller. Immediately before a test, however, the leaf layer was wetted to simulate dew point conditions on track.

The procedure for applying the leaves to the wheel/rail interface was carried out immediately prior to the start of a test. The rig was slowly rotated using the manual control procedure whilst leaves were fed into the contact. The leaves adhered to the rail roller, with some transfer of leaves to the wheel. The process was continued until the circumference of the roller has been covered. Leaves did not uniformly adhere to the surfaces, and as such some further application of leaves was often required. The roller was then rotated whilst a normal load was applied to

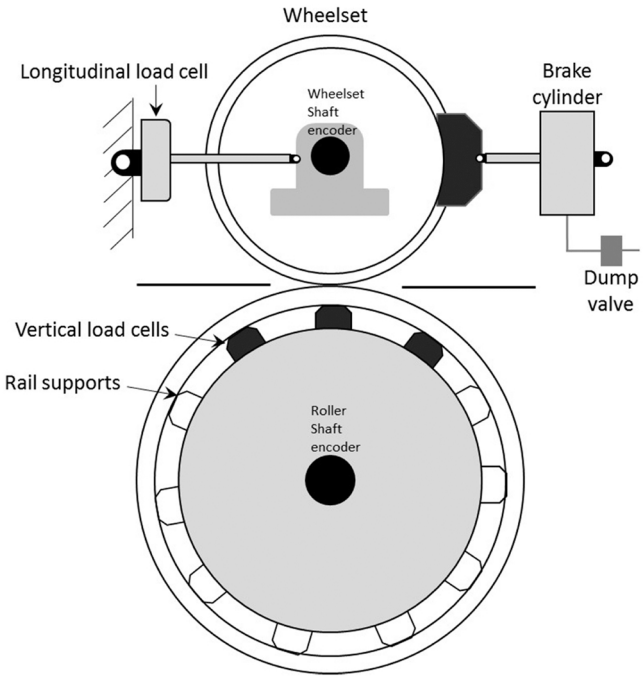

Fig. 6. Instrumentation and Brake Schematic.

Table 1
Applied Wheel Loads and Contact Pressures.

Wheel Load (kN)	Hertzian Contact Stress (MPa)	
	Mean	Maximum
5.5	250	380
11.2	320	480
22.1	400	600
38.1	480	725
60.5	560	845
100.0	665	1000

Table 2
Applied Wheel Loads and Contact Pressures.

Parameter	Contact Condition		
	Dry	Wet	Leaf Layer
Contact Load (kN)	≤ 22.1	≤ 100	≤ 100
Speed (m/s)	≤ 20	≤ 30	≤ 30

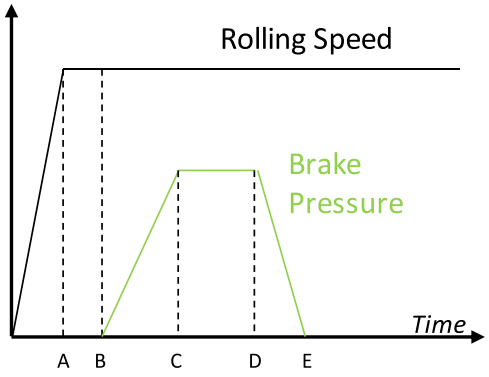

Fig. 7. Typical HAROLD Speed and Braking Profile. Rolling Speed Refers to the Rail Roller Only (wheel velocity would decrease if slip occurs during low adhesion braking).

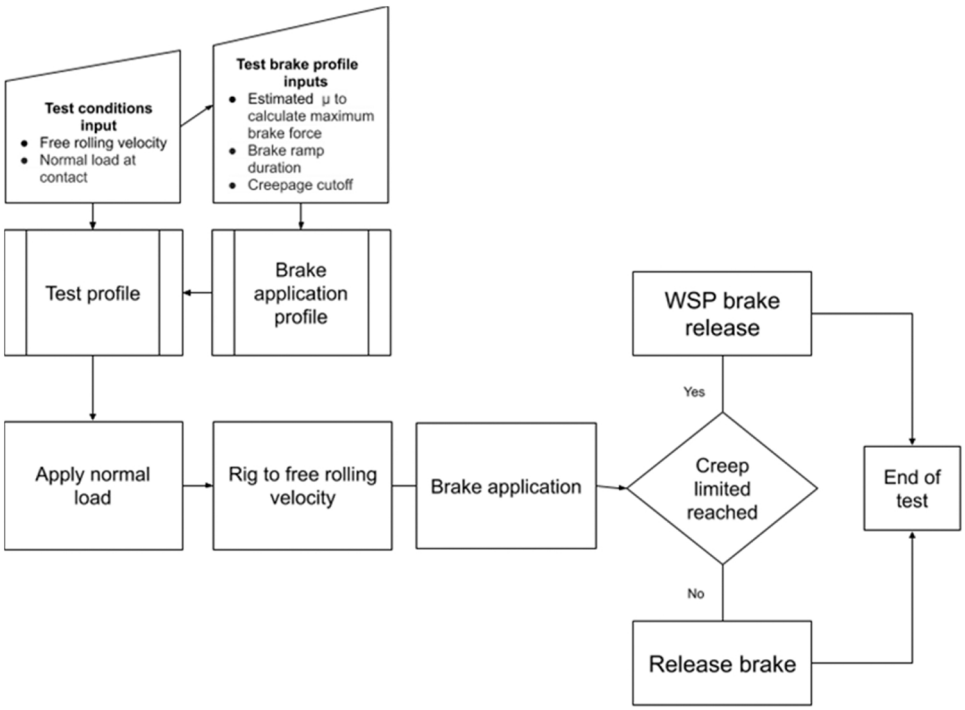

Fig. 8. Flow Chart Showing HAROLD Brake Test Procedure.

Fig. 9. Leaf Film Generation by Hand Application of Leaves.

'bed' the leaves into the surfaces. It was possible in this process that the leaves experienced more wheel passes than would happen in the field. However, the leaf layer showed good durability (i.e. was not worn away before the brake testing) so this was not considered a problem. The consistency of the leaf layer was visually good and further confirmed as the friction levels were measured in the braking tests.

The appearance of the leaf layer on the wheel is shown in Fig. 10. Initially the film had the appearance of compressed leaves on the wheel and/or rail surface. A black leaf film was only visible after the leaf film had undergone a sliding event (during braking in this case). This observation corresponds to work carried out using small scale tests on leaf layer generation [8]. In Fig. 10 it is possible to see a wheel flat that was generated during one of the tests. To avoid this being in the running band for subsequent tests the wheel was moved slightly in the lateral direction.

2.3.3. Test approach

Table 3 shows the stages for carrying out each type of test. The main steps are the same in terms of the rig operation itself (2, 4–6). Differences occur where leaf layers and water were added. Depending on the quantity required, water was applied using a pressurised water sprayer for larger flow rates or a syringe pump for low and more precisely controlled flow rates. Tests were run for a fully flooded contact and then the water application rate was reduced in an attempt to replicate the low adhesion seen in the WILAC project (wheel/rail interface conditions were not comparable to those in the full-scale rig used in the WILAC

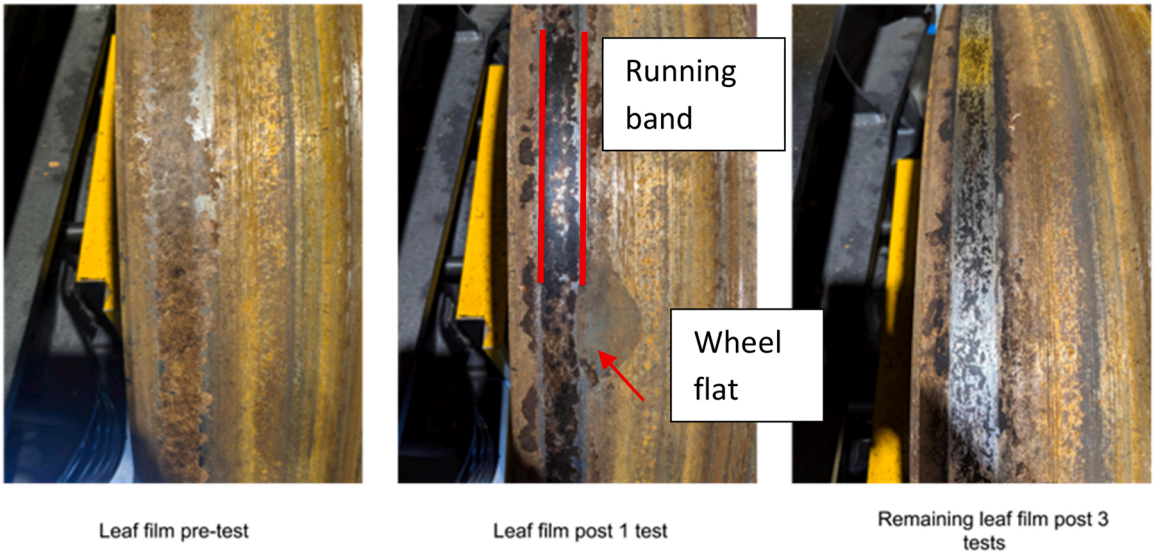

Fig. 10. Example of an Initial Leaf Film on the Wheel and the Remaining Film Post-Tests.

Table 3
Test Stages for Leaf Layer, Wet and Dry Tests.

Stage	Test Type		
	Leaf Layer	Wet	Dry
1	Generate leaf layer		
2	Test rig brought up to specified load and velocity		
3	Application of a small amount of water to wet leaf film surface (uncontrolled spray, but still in the range of amounts to be expected on the railhead in, for example, dew conditions)	Application of water begins	
4	Incremental increase of brake force until wheel slide or maximum brake force application. If set creepage level is exceeded, then WSP dump valve exhausts brake cylinder, braking stops and free rolling is allowed to resume		
5	Roller decelerates to zero velocity (note that the rail rollers are speed controlled so when a brake force is applied to the wheel a torque is applied to the rail roller as well to keep the speed at the desired level)		
6	End of test		

testing, for example (see [1].

2.4. Data processing

The sum of the normal force measured by load cells on the rail roller, as well the sum of the longitudinal force acting on the bogie frame were used to calculate the creep forces.

Shaft encoders provided the rotational speed of the wheel roller and the rail roller. Creepage was calculated based on surface speeds of the rail roller v_R and the wheel v_W according to the following formula:

$$c_x = \frac{(v_R - v_W)}{v_R} \quad (1)$$

A period of 10 s of free rolling after recording of the creep curve was used in each experiment to determine the longitudinal force offset in the measurement assuming that the longitudinal force should be zero in case of free rolling. This period was also used to determine the rotational speeds of the wheel and the rail roller for free rolling where zero longitudinal creep is assumed. The experimental data were low pass filtered with a cut-off frequency of 1.5 Hz and band-stop filtered with middle frequencies ofat 0.245 Hz, 0.365 Hz and 0.848 Hz and their higher order harmonics to remove noise from the measured signal and smoothen the recorded creep curve. The effect of the filtering process for two recordings is shown in Fig. 11(b) and (d).

Fig. 11 shows creep force data in dry and leaf contaminated condition. Fig. 11(a) shows that in dry condition the braking force is increased linearly over a period of 20 s. At a certain point the rotational speed of the wheelset decreases quickly (increasing creep, labelled with "I"). When the WSP releases the brake the wheelset reaccelerates (decreasing creep, labelled with "D") until pure rolling resumes. In the case of leaf contamination only a small braking force triggers the sliding event, as can be seen in Fig. 11(c). The duration of the sliding event varies but is typically less than 5 s. Usually the increasing creep part "I" of the recording, representing loss of adhesion, differs from the decreasing creep part "D" representing re-adhesion (see Fig. 11(b)). In the figures that follow only the increasing creep part "I" (see Fig. 11(b) and (d)) of the recording is reported.

3. Results and discussion

Over 100 tests were carried out within the parameter ranges specified in Section 2.2. Not all are presented within this section and some extra material is included as "Supplementary Data".

3.1. Dry conditions

Figs. 12 and 13 show results for dry contact conditions. Through all the graphs, T refers to tractive force and N to normal force, with T/N being the traction coefficient. The creep curve displays an initial steep increase with a maximum traction coefficient of approximately 0.4–0.5, followed by a decrease in adhesion with increasing creep. This is similar to creep curves reported in literature in full-scale tests (see for example [[3,19].

Previous work by [14]] showed that speed has little effect on traction coefficient below 300 km/h (83 m/s) and [19]] saw the same in their tests up to 70 km/h. In this work the speeds for dry tests ranged from 18 km/h (5 m/s) to 72 km/h (20 m/s) so the lack of variation due to speed is not unexpected.

A reduction of the traction coefficient at high creep with increasing load is observed (see Fig. 13) although the significance of this needs to be clarified with further tests. Additional results for 5 m/s rolling speed at varying loads are included as supplementary data (Fig. S1) where the relationship is unclear. Previous tests carried out by [19]] also showed a reduction in friction at some speeds, but not others.

3.2. Wet conditions

Wet experiments were performed in two ways:

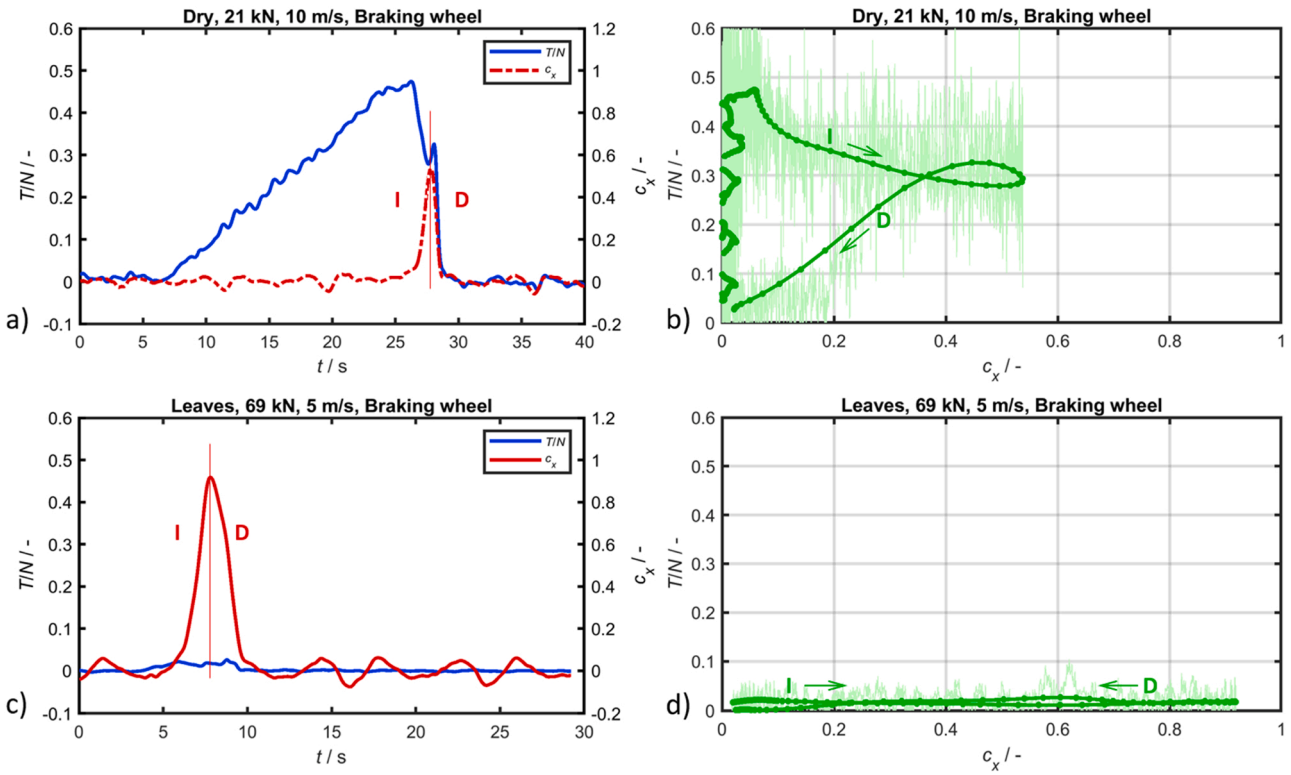

Fig. 11. a) Adhesion and Creep as a Function of Time, Dry Condition, 21 kN Contact Force, 10 m/s Rolling Speed; b) Corresponding Creep Force Curve; Thick Line: Filtered Data, Thin Lines/Background: Unfiltered Data; c) Adhesion and Creep as a Function of Time with Leaf Layer, 69 kN Normal Contact Force, 5 m/s Rolling Speed; d) Corresponding Creep Force Curve; Thick Line: Filtered Data, Thin Lines/Background: Unfiltered Data (note that $c_x = 1$ represents a locked wheel; "I" indicates the Increasing Creepage (decreasing rotational speed of wheel); "D" Indicates Decreasing Creepage (increasing rotational speed / reacceleration of wheel) in the Experiment; Filled Circles in b) and d) are Plotted Every 0.05 s).

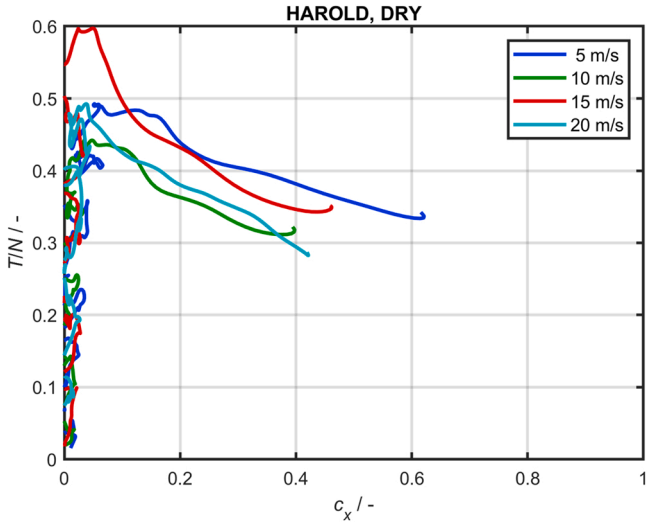

Fig. 12. Creep Force Behaviour in Dry Conditions with Variation of Rolling Speed at 11 kN Nominal Wheel Load (note: $c_x = 1$ in braking represents a locked wheel).

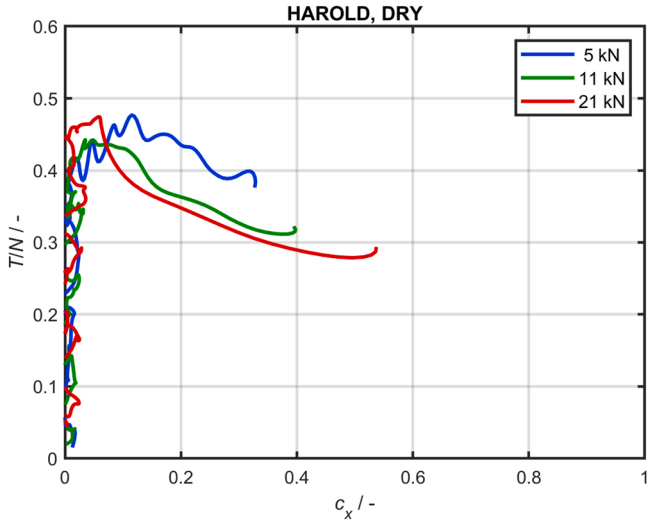

Fig. 13. Creep Force Behaviour in Dry Conditions with Variation of Wheel Load at 10 m/s Rolling Speed.

- continuous application of water spray during the creep curve measurement at uncontrolled (larger) water flow rates
- continuous application of water spray at lower, controlled water flow rates.

If no water flow rate is stated, water has been applied in an uncontrolled manner at larger flow rates (flooded wet conditions).

Fig. 14 shows creep curves for flooded wet contact conditions at 22 kN nominal wheel load for varying rolling speeds. There is a steep initial increase of adhesion with creep up to a value of approximately 0.15, followed by a gentler increase of adhesion up to approximately 0.30. An increase of adhesion with increasing rolling speed is observed.

The measurements at 5 m/s (18 km/h) and 10 m/s (36 km/h) rolling speed in Fig. 14 show a fast increase of creep at the transition to full slip conditions. These events are caused by exceeding the available adhesion

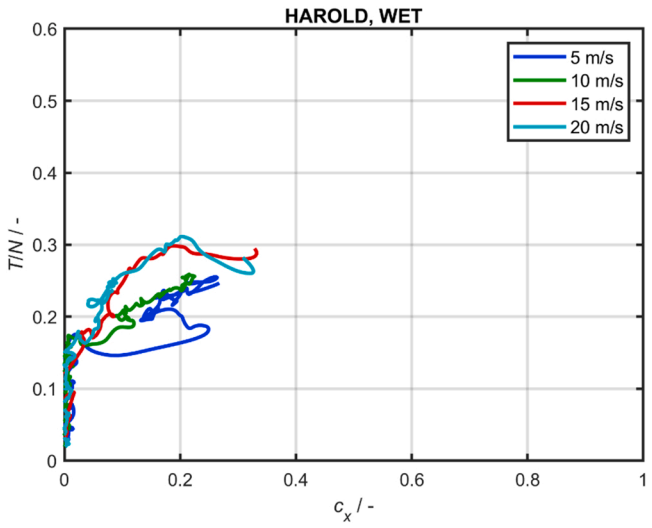

Fig. 14. Creep Force Behaviour with Variation of Rolling Speed at 22 kN Nominal Wheel Load for Flooded Wet Contact Conditions.

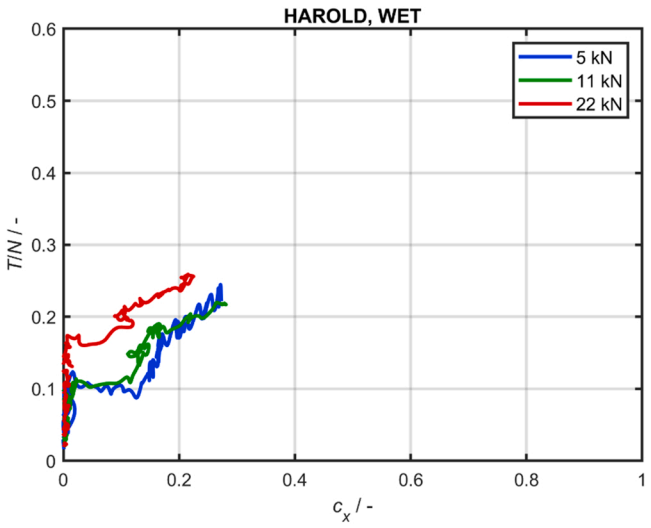

Fig. 15. Creep Force Behaviour with Variation of Wheel Load at 10 m/s Rolling Speed for Flooded Wet Contact Conditions.

in the contact patch that causes the wheelset to decelerate quickly due to the constant braking force that is applied to the wheelset. Similar results (which are included as supplementary data (Fig. S2)) were seen for the same rolling speeds at 11 kN wheel load.

Previous work on wet contacts at full-scale has shown similar shape creep curves to the those achieved here [3,19]. A sharp rise at low slip reaching a maximum and staying constant from there on or reducing slightly, but not as much as was seen in dry tests. However, all other work has shown a decrease in the traction coefficient with increasing speed which is not evident in this work. It should be noted, however, that in previous work test speeds were up to 400 km/h and the combination of operational and surface parameters put the interface into the hydrodynamic lubrication regime (i.e. surface separation was occurring), as evidenced by the low friction levels achieved (below 0.05 in some cases). In this regime surface speed has a strong influence on friction which is not the case for the boundary lubrication regime (i.e. with partial metal-to-metal contact) that the current tests are operating in, where friction levels are much higher (0.2–0.4). Previous work carried out at similar speeds on full-scale test apparatus has shown similar friction levels. For example, [3]], reported a peak traction coefficient of around 0.22 for 40 km/h which compares well with the data in Fig. 14. The difference between 5 and 10 m/s and 15 and 20 m/s shown in Fig. 14 could have been caused by the slip increase that occurred, because otherwise the initial rate of increase in coefficient of traction was similar for all speeds. This was a result of the rig operation and control rather than the interface though.

Fig. 15 shows that increasing the normal load raises adhesion for a 10 m/s rolling speed. However, the increase of adhesion with increasing wheel load is less pronounced in data with other rolling speeds (additional results for 5 m/s rolling speed and 20 m/s rolling speed are included as supplementary data (Figs. S3 and S4 respectively). Typically, data from other full-scale tests shows that adhesion decreases with increasing load [3]. However, it should again be highlighted that this testing was carried out at much higher speed and was more likely to have been in a hydrodynamic regime where increasing load on a full fluid film has a different effect to that on a contact in a boundary lubrication regime. Tests carried out at similar speeds to those used in the current work [19] do not show a clear trend, reflecting what has been shown in the current tests. Work carried out with water lubrication using a pin-on-disc test showed increasing friction as load was increased [20]. The increasing load would have increased the real contact area as well as possibly squeezing out the water from the wheel-rail contact.

Repeatability between two consecutive test series in flooded, wet conditions is good as shown in Fig. 16. The experiments have been performed in the order as they appear in the legend within a time difference of approximately 30 min

Increasing the rate of water application from 25 μl/s to 1460 μl/s at 5 m/s rolling speed causes a reduction of the adhesion for creepage up to approximately 0.3 (see Fig. 17). The reduction is in line with observations made during previous work [3] (additional results for 5 kN wheel load at 5 m/s rolling speed are included in supplementary data (Fig. S5)).

The lubrication regime, while affected by load and speed is also influenced greatly by the surface roughness.

3.3. Leaf layers

Experimental results with leaves are reported for fully contaminated conditions, unless otherwise stated. The leaf layer was created before cycle 1. Adhesion results are repeatable for consecutive recordings on the same leaf layer as long as full contamination prevails, as shown in Fig. 18 for cycles 1–4 recorded with 100 kN nominal wheel load at 10 m/s rolling speed (note that the maximum value of the coefficient of adhesion shown in the figures has been reduced to 0.2 in this section).

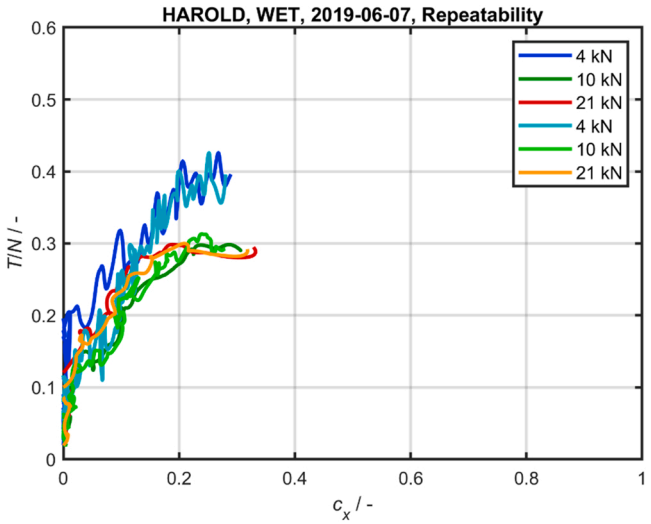

Fig. 16. Repeatability of Two Consecutive Test Series; Variation of Wheel Load at 15 m/s Rolling Speed for Flooded Wet Contact Conditions.

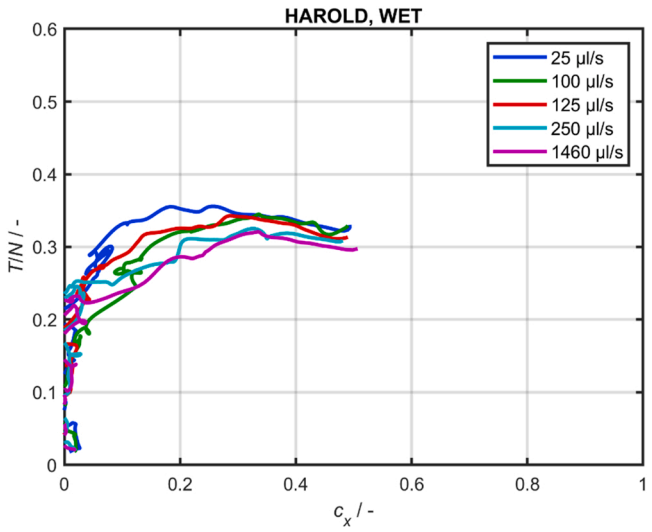

Fig. 17. Creep Force Behaviour with Variation of Water Flow Rate at 22 kN Nominal Wheel Load and 5 m/s Rolling Speed.

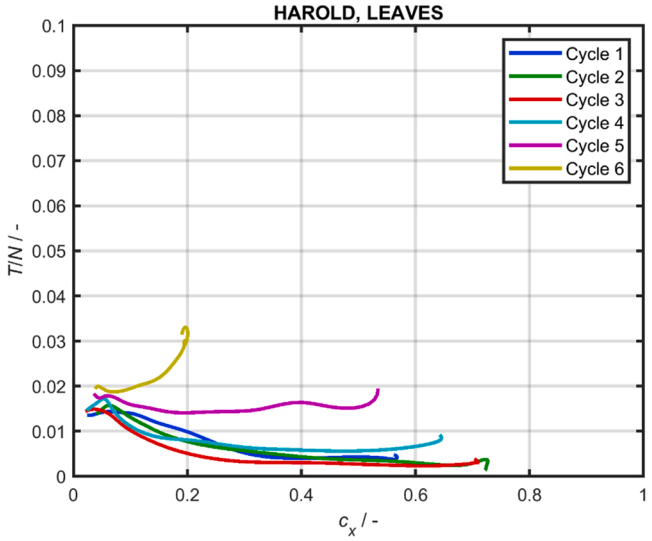

Fig. 18. Repeatability of Creep Force Measurements for Consecutive Creep Curve Recordings after Creation of the Leaf Layer before Cycle 1 for 100 kN Nominal Wheel Load at 10 m/s Rolling Speed.

Leaf contamination resulted in ultra-low adhesion with maximum values in the range of 0.01. These are in the range seen in small scale tests [2,6]. To put these values in context, passenger train service brake applications provide decelerations in the range 3%g to 9%g and therefore require a traction coefficient at the wheel-rail interface of approximately 0.03–0.09 (the relationship is not exact). The traction coefficients found in these results are at or below the very lowest end of the range typically reported [21] for skis running on snow or ice (typically 0.02 – 0.04).

Looking at the wheel surfaces shown in Fig. 10 after one and three cycles, it is clear that the layer has started to be removed by cycle 3, but it is not until cycle 5 that this process is having an effect on friction levels. Even then, the friction increase is still not that large. This could be a significant observation for understanding how effective rail cleaning needs to be.

The number of sliding events which could be carried out after the preparation of the leaf layer until a noticeable increase of adhesion is observed varies from test to test. This is shown in Fig. 19 where an

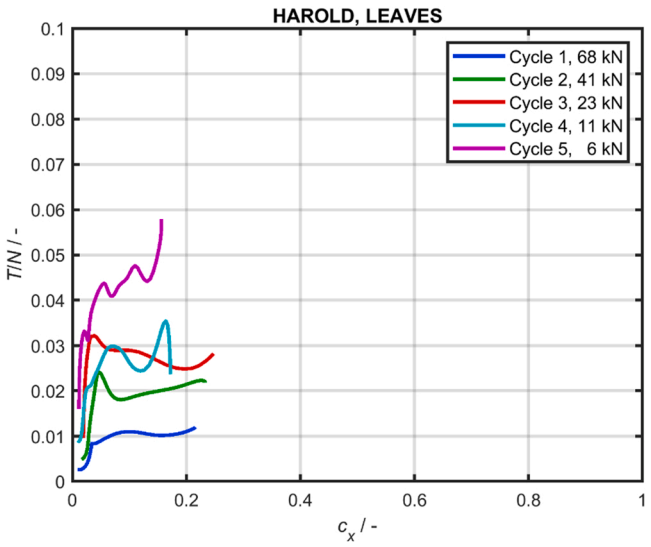

Fig. 19. Increase of Adhesion due to Degradation/Partial Removal of the Leaf Layer for Consecutive Cycles at 5 m/s Rolling Speed while Wheel load was Decreased from 68 kN (blue) to 6 kN (magenta).

increase in adhesion value is observed with each sliding event.

The ultra-low values of friction do not change noticeably with rolling speed, as shown in Fig. 20 for a wheel load of 60 kN.

Fig. 21 shows that wheel load does not have an influence on the adhesion value in fully leaf-contaminated conditions. Maximum adhesion values observed are approximately 0.01 at 10 m/s rolling speed for wheel loads varying between 23 kN and 94 kN (additional results for varying wheel loads at 5 m/s and 30 m/s rolling speed are included as supplementary data (Figs. S6 and S7 respectively)).

4. Conclusions

The aim of the work was to carry out leaf layer brake tests on the Huddersfield Adhesion and Rolling Contact Laboratory Dynamics Rig (HAROLD) full-scale test rig with leaf layers to generate creep curves for a leaf contamination condition. These were to be used as standalone information for use in modelling of train braking performance as well as forming the basis of a tool for giving creep curves for a range of wheel/

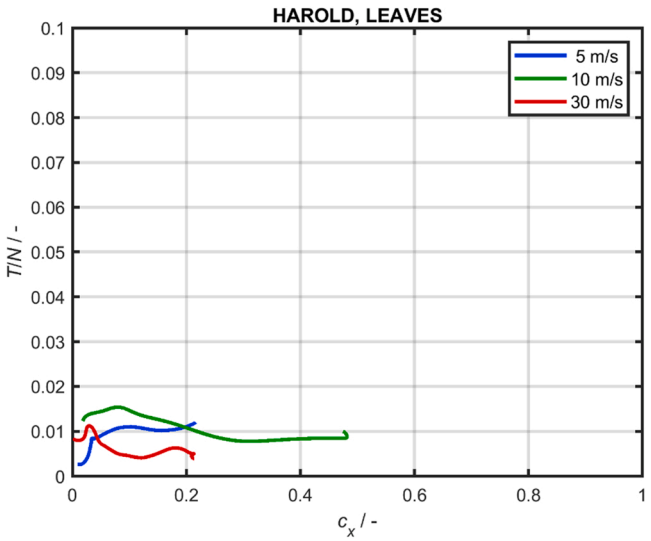

Fig. 20. Creep Force Behaviour with Leaf Contamination and Variation of Rolling Speed at Nominal Wheel Load of 60 kN.

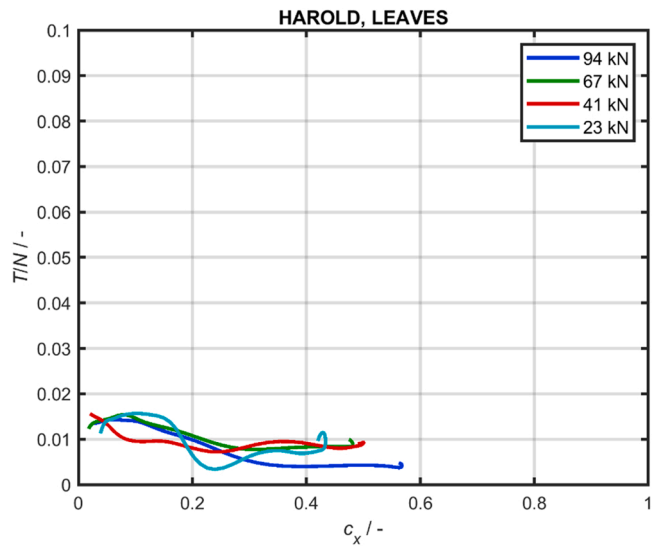

Fig. 21. Creep Force Behaviour with Leaf Contamination and Variation of Wheel Load at 10 m/s Rolling Speed.

rail interface and leaf contamination conditions which will be outlined in a future paper.

New instrumentation and control methods were developed to give the HAROLD rig new capability to measure friction and carry out tests to generate creep curves. Methods for creating leaf layers were also successfully developed. The leaf testing has generated a unique creep force data set not previously available for full-scale test conditions. It has also shown the importance of the shear induced in the brake tests for creating the black, well-bonded leaf layer. It was found in the tests that ultra-low adhesion was achieved in all tests with leaves regardless of load applied and speed. The friction remained low for a number of braking events, even when the layer had been partially removed.

The test method provides a means to develop improved modelling of leaf contaminated contacts to understand the effects on train performance, especially braking. It also provides a platform for testing mitigation methods for dealing with leaf contamination. The leaf layers created can also be analysed to understand the properties of the layers better.

CRediT authorship contribution statement

Roger Lewis: Supervisor; Conceptualisation; Project Administration; Writing – review and editing, **Klaus Six;** Conceptualisation; Writing – review and editing, **Gerald Trummer:** Supervisor; Conceptualisation; Project Administration; Writing – review and editing, **Julian Stow:** Supervisor; Conceptualisation; Project Administration; Writing – review and editing. **Hamid Alturbeh;** Investigation; Methodology; Writing – original draft, **Luke Buckley-Johnstone:** Investigation; Methodology; Writing – original draft, **Barnaby Bryce:** Investigation; Methodology, **Phil Shackleton:** Investigation; Methodology.

Declaration of Competing Interest

The authors declare the following financial interests/personal relationships which may be considered as potential competing interests: Roger Lewis reports financial support was provided by Railway Safety and Standards Board. Roger Lewis reports a relationship with Railway Safety and Standards Board that includes: funding grants.

Data Availability

Data will be made available on request.

Acknowledgements

This work was funded by the Rail Safety and Standards Board (RSSB) within the project T1149. The work was also supported by the EPSRC Programme Grant “Friction: The Tribology Enigma” (EP/R001766/1). G. Trummer and K. Six gratefully acknowledge additional funding within the COMET K2 Competence Centers for Excellent Technologies from the Austrian Federal Ministry for Climate Action (BMK), the Austrian Federal Ministry for Digital and Economic Affairs (BMDW), the Province of Styria (Dept. 12), and the Styrian Business Promotion Agency (SFG). The Austrian Research Promotion Agency (FFG) has been authorized for the program management. For the purpose of open access, the author has applied a Creative Commons Attribution (CC BY) license to any Author Accepted Manuscript version arising. The authors confirm that this is original work and the paper has not been submitted elsewhere for publication.

Appendix A. Supporting information

Supplementary data associated with this article can be found in the online version at doi:10.1016/j.triboint.2023.108529.

References

[1] Buckley-Johnstone L, Trummer G, Voltr P, Six K, Lewis R. Full-scale testing of low adhesion effects with small amounts of water in the wheel/rail interface. Tribology Int 2020;141:105907.
[2] Cann PM. The "Leaves on the Line" problem - a study of leaf residue film formation and lubricity under laboratory test conditions. Tribology Lett 2006;24:151–8.
[3] Chang C, Chen B, Cai Y, Wang J. An experimental study of high speed wheel-rail adhesion characteristics in wet condition on full scale roller rig. Wear 2019; 440–441:203092.
[4] Chen, H. Wheel slip/slide and low adhesion caused by fallen leaves. Wear 2020; 446–447:203187.
[5] Evans M, Skipper WA, Buckley-Johnstone L, Meierhofer A, Six K, Lewis R. The development of a high pressure torsion test methodology for simulating wheel/rail contacts. Tribology Int 2021;156:106842.
[6] Gallardo-Hernandez EA, Lewis R. Twin disc assessment of wheel/rail adhesion. Wear 2008;265:1309–16.
[7] Ishizaka K, White B, Watson M, Lewis SR, Lewis R. Influence of temperature on adhesion coefficient and bonding strength of leaf films: a twin disc study. Wear 2020;454–455:203330.
[8] Ishizaka K, Lewis SR, Hammond D, Lewis R. Chemistry of black leaf films synthesised with rail steels and its influence on low friction mechanism. RSC Adv 2019;8:32506–21.
[9] Ishizaka K, Lewis SR, Lewis R. The low adhesion problem due to leaf contamination in the wheel/rail contact: bonding and low adhesion mechanisms. Wear 2017; 378–379:183–97.
[10] Ishizaka K. The Low Adhesion Problem due to Leaf Contamination in the Wheel/Rail Contact: Bonding and Low Adhesion Mechanisms, PhD Thesis. The University of Sheffield; 2019.
[11] Lanigan J, Krier P, Buckley-Johnstone L, White B, Ferriday P, Lewis R. Field trials of a methodology for locomotive brake testing to assess friction enhancement in the wheel/rail interface using a representative leaf layer. J Rail Rapid Transit Proc IMechE Part F 2021;235:1053–64.
[12] Lewis SR, Lewis R, Cotter J, Lu X, Eadie DT. A new method for the assessment of traction enhancers and the generation of organic layers in a twin-disc machine. Wear 2016;366–367:258–67.
[13] Lewis, R., Evans, M.E., Six, K., Meierhofer, A., Stock, R., Gutsulyak, D., 2022, Top-of-Rail Friction Modifier Performance Assessment: High Pressure Torsion Testing; Creep Force Modelling and Field Validation, Proceedings of CM2022, 12th International Conference on Contact Mechanics and Wear of Rail/Wheel Systems, Melbourne, Australia, 4–8 September 2022.
[14] Ohyama, T., Maruyama, H., 1983, Traction and Slip at Higher Rolling Speeds - Some Experiments under Dry Friction and Water Lubrication, Proceedings of Contact and Wear of the Rail/Wheel System, July, 1982, Vancouver, Canada, pp. 395–418.
[15] Skipper, W., Meierhofer, A., Chalisey, A., Six, K., Lewis, R., 2022, Generation of Sanded Creep Curves using the Extended Creep Force Model with High Pressure Torsion Data, Proceedings of CM2022, 12th International Conference on Contact Mechanics and Wear of Rail/Wheel Systems, Melbourne, Australia, 4–8 September 2022.

[16] Trummer G, Buckley-Johnstone L, Voltr P, Meierhofer A, Lewis R, Six K. Wheel-rail creep force model for predicting water induced low adhesion phenomena. Tribology Int 2017;109:409–15.
[17] Vollebregt E, Six K, Polach O. Challenges and progress in the understanding and modelling of the wheel–rail creep forces. Veh Syst Dyn 2021;59:1026–68.
[18] Watson M, White B, Lanigan J, Slatter T, Lewis R. The composition and friction reducing properties of leaf layers. Proc R Soc 2020;476:20200057.
[19] Zhang W, Chen J, Wu X, Jin X. Wheel/rail adhesion and analysis by using full scale roller rig. Wear 2002;253:82–8.
[20] Zhang H, Zhou G, Zhong P, Wu K, Ding X. Experimental investigation on stribeck curves of different elastic modulus materials under oil and water lubrication conditions. Ind Lubr Tribology 2020;72(No. 6):805–10.
[21] W. Nachbauer, P. Kaps, M. Hasler, M. Mössner, 2016, Friction Between Ski and Snow, F. Braghin et al. (eds.), The Engineering Approach to Winter Sports, Chapter 2, pp26 – 30.